

AdditiveLLM: Large Language Models Predict Defects in Metals Additive Manufacturing

Peter Pak[†] and Amir Barati Farimani^{*,†,‡}

[†] *Department of Mechanical Engineering, Carnegie Mellon University, Pittsburgh, PA, USA*

[‡] *Machine Learning Department, Carnegie Mellon University, Pittsburgh, PA, USA*

E-mail: barati@cmu.edu

Abstract

In this work we investigate the ability of large language models to predict additive manufacturing defect regimes given a set of process parameter inputs. For this task we utilize a process parameter defect dataset to fine-tune a collection of models, titled *AdditiveLLM*, for the purpose of predicting potential defect regimes including *Keyholing*, *Lack of Fusion*, and *Balling*. We compare different methods of input formatting in order to gauge the model’s performance to correctly predict defect regimes on our sparse *Baseline* dataset and our natural language *Prompt* dataset. The model displays robust predictive capability, achieving an accuracy of 93% when asked to provide the defect regimes associated with a set of process parameters. The incorporation of natural language input further simplifies the task of process parameters selection, enabling users to identify optimal settings specific to their build.

1 Introduction

Within the process of Laser Powder Bed Fusion (L-PBF), the selection of optimal process parameters remains a key factor in the fabrication of defect free parts.^{1,2} This is achieved

by avoiding the combination of process parameters that can potentially lead to melt pool characteristics resulting in either unfused powder or void initiation causing defect formation within the final part. The following defect regimes of *Keyholing*, *Balling*, and *Lack of Fusion (LoF)* describe the expected melt pool characteristics seen at a given combination of process parameters.² These defect regimes can be estimated by methods such as experimental observation,³ computational simulation,⁴ or surrogate modeling.⁵

Equations 1 - 3 provide criterions dependent on melt pool dimensions and process parameters where when satisfied are expected to avoid their respective defect regimes. Melt pool conditions such as *Keyholing* do not inherently cause defects, rather it is fluctuations and collapse of the rear wall that generates voids leading to the formation of pores.⁶ However due to the inaccessibility of *in-situ* cross-sectional melt pool analysis, the formation of *Keyhole* defects is often approximated with Equation 1, where width to depth ratios below threshold are likely to result in keyhole porosity.⁷ For defects resulting from *Lack of Fusion*, the ratio of hatch spacing and melt pool width along with layer height and depth are evaluated to ascertain the potential formation of porosity.⁸ The criterion for full melting across subsequent melt pools is defined as Equation 2 where computed values above the threshold can result in unfused powder.^{8,9} *Balling* defects occur due to the hydrodynamic capillary instabilities that occur during high scan speeds and the resulting grooves along the sides of the melt pool result in formation of voids if not remelted.¹⁰ An approximation for the occurrence of this phenomenon is calculated by comparing the length and width of the melt pool (Eq. 3). A ratio above π can indicate the presence of balling, though this value can range depending on the material.⁷

$$\frac{Width}{Depth} > 1.5 \quad (1)$$

$$\left(\frac{Hatch\ Spacing}{Width}\right)^2 + \left(\frac{Layer\ Height}{Depth}\right)^2 \leq 1 \quad (2)$$

$$\frac{Length}{Width} < \pi \quad (3)$$

The selection of optimal process parameters often requires extensive domain knowledge of the various domains within the L-PBF process, ranging from material properties to experimental trials. Large Language Models (LLM) present a suitable solution for encapsulating these domains and have demonstrated significant success in reasoning and generating precise responses based on a given prompt.¹¹⁻¹⁶ LLMs are able to understand textual descriptions of experimental results and respective context which enables its application as a more human accessible research tool in a wide domain of fields ranging from chemical engineering to robotics.¹⁷⁻²⁷ Implementations such as LLAMA,^{11,12,28} GPT,¹⁵ T5²⁹ and BERT¹⁴ provide a foundation for general purpose use where it can then be fine-tuned for a specific downstream application.

The Bidirectional Encoder Representations from Transformers (BERT)¹⁴ model is one way to architect a LLM and has garnered much attention creating the base for extensions such as RoBERTa (**R**obustly **o**ptimized **B**ERT Approach),¹⁶ ALBERT (**A** Lite **B**ERT),³⁰ and DistilBERT.³¹ These models which improves upon the existing implementation by either employing specific training strategies such as a dataset, batch sizes, sequence lengths, and hyperparameter optimization.^{16,30,31} The BERT model differs from the classical masked language model in that it randomly masks its input tokens in order to predict the original vocabulary based solely through context.¹⁴ The bidirectional approach for representing inputs that BERT takes allows for the model to consider a more complete context window of a given sequence, providing tokens on both sides of an applied mask.¹⁴ This is contrast to the unidirectional approach that models such as GPT take in order to more align closer to the sequential nature of text generation.³²

In this work we propose AdditiveLLM, a comparison of large language models fine-tuned on experimental and simulation based L-PBF melt pool data that able to predict potential defects given a combination of process parameters. We focus upon fine-tuning several mod-

els including: DistilBERT,³¹ SciBERT,³³ LLama 3.2,³⁴ and T5.³⁵ Our selection of models utilize the smaller parameter set variants as this best suits our need for an efficient and lightweight model for specific inferences regarding defect regimes in L-PBF Additive Manufacturing. This approach infers upon the corpus of L-PBF melt pool data formatted as a set of process parameters inputs and defect classification labels. The model predictions provide a classification to a combination of potential defect regimes of *Keyholing*, *Lack of Fusion*, *Balling*, and *None* (for the case where no defects exist). Through inference the models are able to quickly provide insight on potential defects given a specific parameter combination without the need to perform additional simulations or experimental builds.

2 Methodology

2.1 Task

Given an input text sequence outlining a L-PBF build process with descriptions of process parameters such as material, power, and velocity; AdditiveLLM aims to predict the most appropriate combination of defect classifications that is likely to occur. The defect classifications of *Keyholing*, *Lack of Fusion*, *Balling*, and *None* are one-hot encoded and provide a set of labels for the multi-label classification task. The *Baseline* (Figure 5) and *Prompt* (Figure 6) datasets provide structure to the input in the form of order dependent process parameters delineated with [SEP] separation tokens or queries regarding process parameters in the format of natural language respectively. The *Prompt* dataset aims to capture the behavior of the unstructured input expected from a user while the *Baseline* dataset aims to definitively capture each process parameter. These distinct approaches allow for a more flexible use case for the models as the user is able to specifically tune inputs specific to their use case.

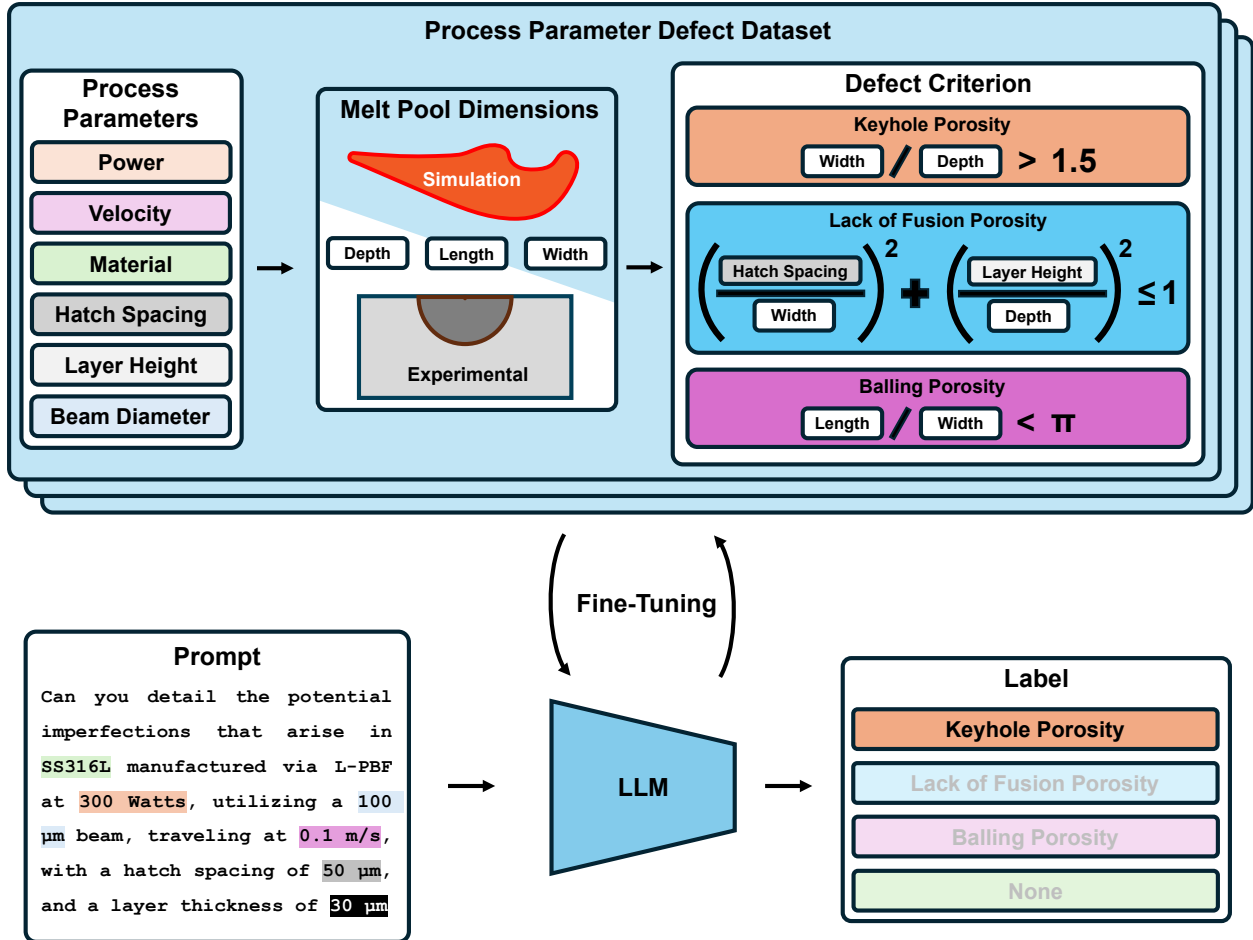


Figure 1: A series of LLM models are fine-tuned with a process parameter defect dataset generated from experimental results obtained from literature and simulations performed with FLOW-3D. The corresponding melt pool dimensions are used in the computation of defect criteria used as classifications labels for a specific process parameter combination. A prompt which incorporates the process parameters is provided as input to the model which in turn predicts the potential defect classification.

2.2 Dataset

The dataset is compiled from literature and simulation values that provide either melt pool dimensional measurements or corresponding defect classifications from a set of process parameters. These process parameters include `material`, `power`, `velocity`, `beam_diameter`, `hatch_spacing`, and `layer_height` and their corresponding units. The majority of the data only consists melt pool dimensional measurements and these data points are processed into defect classifications using estimations for *Keyholing* (Eq. 1), *Lack of Fusion*(Eq. 2), and

Balling (Eq. 3).

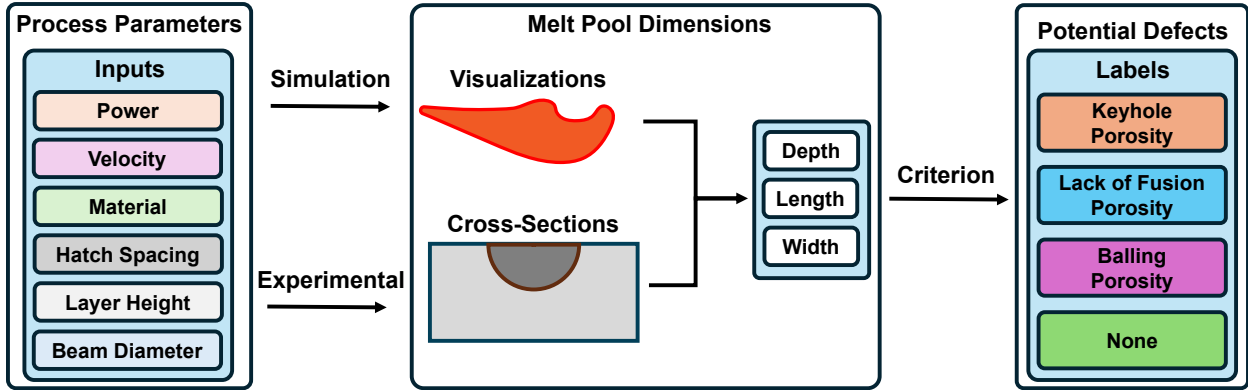


Figure 2: Melt pool dimensions dependent on the corresponding process parameters are obtained through either experimental cross-sectional measurements or computational fluid dynamic simulations. The obtained depth, length, and width, dimensions, pass through a set of criteria that determine the potential defects that would arise from the combination of process parameters.

A number of sources were used for our dataset which include literature and simulation data points curated by *Akbari et al.* in *MeltpoolNet*³⁶ and our own simulations obtained using FLOW-3D.³⁷ (Figure 2) This amounts to a total of 2779 collected data points spanning over 20 different materials, primarily consisting of Ti-6Al-4V and Stainless Steel 316L. With these sources, the dataset is comprised of over 20 different materials varying with powers and velocity values ranging from 25 W to 5000 W and 1 mm/s to 2000 mm/s respectively.

The models were fine-tuned using this data using one hot encoded labels to denote classifications of *Keyhole*, *Lack of Fusion*, *Balling*, and *None*. The label is formatted to be compatible with a multi-label classification task since these defect regimes are not mutually exclusive to one another. An example of two valid labels would be in the case of a melt pool in keyhole mode creating pores while still producing lack of fusion defects due to excessive layer height. The text input for the dataset is formatted in two separate approaches, the first being *Baseline* (Figure 5) structure relying on the bare minimum amount of data and the second as the *Prompt* (Figure 6) arrangement resembling inputs more akin to natural language.

2.2.1 Data Generation and Split

The dataset consists of simulation and experimental data derived from sources such as *Melt-poolNet*³⁶ (`meltpoolclassification.csv`, `meltpoolgeometry.csv`) and a number of our own FLOW-3D³⁷ simulations (`dimensions_ti64.pkl` and `dimensions_ss316l_10_micron.csv`). The `meltpoolclassification.csv` provides the direct defect classification of a combination of process parameters, however in cases where only the melt pool dimensions are provided, the defect classifications are obtained using their respective criterions. This data was further augmented by analyzing the *Lack of Fusion* defect criterion on 20 different layer heights and hatch spacings ranging from 0 μm to 950 μm with the assumption that the melt pool’s width and depth remain the same. Each of these individual files, all of the entries are shuffled and split to 75%, 15%, and 10% for the train, test, and validation datasets respectively.

2.2.2 Baseline Dataset

The *Baseline* configuration of our dataset seeks to provide the minimum input data necessary to fine-tune each model. This is done by utilizing the [SEP] token to indicate the distinction between ordered process parameters of `material`, `power`, `velocity`, `beam_diameter`, `hatch_spacing`, and `layer_height` (Figure 5). The streamlined text input of just the process parameters aims to provide the model only the essential parameters to generate a prediction. This amounted to a total of 724,764 distinct input-label pair combinations with the 75%, 15%, 10% train, test, validation split including 543,573, 108,715, and 72,476 respectively.

2.2.3 Prompt Dataset

The *Prompt* dataset consists of the same process parameter inputs but structured in a way that more closely resembles natural language. This was achieved through the use of ChatGPT to generate 100 unique prompt templates querying for the potential defect associated with a combination of process parameters. The template provides the same fields as the

Baseline configuration to generate a set of text inputs for each set of process parameter combinations within the data (Figure 6). With the 75%, 15%, and 10% respectively set to the train, test, and validation split, the 100 unique prompt templates are also split accordingly such that there are either 75, 15, or 10 unique prompts generated from each set of process parameters depending on the split of the dataset. This increases the input-label pair of the dataset by 100x to over 70 million distinct pairs over all train, test, and validation splits.

2.3 Large Language Models

2.3.1 DistilBERT

DistilBERT is a distilled implementation of the BERT model for the purposes of fine tuning developed by researchers at HuggingFace.³¹ DistilBERT achieves a 40% reduction in model size (66 million parameters) compared to the original BERT (110 million parameters) model while retaining 97% of the language understanding capability and gaining a 60% increase in training speed.³¹ This model is a suitable candidate for obtaining preliminary insights and evaluating the feasibility of implementing a BERT-based inference approach for process parameter dependent defects. The training process for the classification head a batch-size of 512 and a learning rate of 2E-5.

2.3.2 SciBERT

SciBERT is a specialized implementation of the 110 million parameter BERT model¹⁴ pre-trained on large-scale scientific data including numerous publications from computer science to biomedical research.³³ With a dataset of over 1.14 million papers, the authors are able to pretrain the BERT implementation on a corpus of text with the use of domain specific vocabulary allowing better representation of scientific terms and symbols through their SciVocab vocabulary library.³³ When evaluated on Natural Language Processing (NLP) tasks regarding Named Entity Recognition (NER), PICO Extraction (PICO), and Relation Classification

(REL); SciBERT surpasses State Of The Art (SOTA) performance, establishing its proficiency in comprehending and executing scientific tasks.³³ For this reason, we believe that defect classification would be a suitable task for a finetuned implementation of SciBERT with our *Baseline* and *Prompt* datasets. This model’s classification head was fine-tuned with a batch size of 256 and a learning rate of 2E-5.

2.3.3 Llama 3

Llama 3 is the latest iteration of LLMs developed by the AI team at Meta.²⁸ In comparison to the previous implementations, Llama 3 is trained on a much larger dataset of 15 trillion tokens, boasts a larger context window of up to 128K tokens, and consists of 405 billion parameters for its largest model.^{11,12,28} For our implementations we utilize Llama-3.2-1B, a 1 billion parameter implementation of the the Llama 3 model that incorporates the logits of the 8 billion and 70 billion parameter Llama 3.1 models during pretraining in order to retain a majority of their performance while reducing the hardware requirements for finetuning.³⁴ This model was fine-tuned with a batch size of 512 and a learning rate of 2E-5.

2.3.4 T5

Text to Text Transfer Transformer (T5) is an encoder-decoder large language model developed by Google specializing in simple text to text tasks such as translation, summarization, and sentiment analysis.²⁹ Variations of this model extend up to 11 billion parameters and for our experiment we utilize T5-Small³⁵ consisting of 60 million parameters for its efficient training speed and performance on a specialized task such as defect classification.^{29,35} This model was fine-tuned with a batch size of 512 and a learning rate of 1E-4 following the guidelines outlined in the documentation.³⁸

2.4 Training

Each of the LLM models were attached with a classification head and fine-tuned using the *Baseline* and the *Prompt* dataset. In each case the weights of the LLM model remain unfrozen and were trained along with the classification head for up to 25 epochs for *Baseline* fine-tuning and 2 epochs for *Prompt* fine-tuning. Models fine-tuned on the *Prompt* dataset were done so for a shorter number of epochs due to the lengthy training duration resulting from the dataset being 100x larger than that of the *Baseline*. Binary cross entropy was used as the loss function for this multi-label classification task and the inputs were tokenized with each LLM’s respective tokenizer used in pretraining. The models were fine-tuned on various machines with GPU resources of Nvidia RTX A6000 with 48 GiB of memory and Nvidia RTX 2080Ti with 11 GiB of memory dependent on which were available. The Llama-3.2-1B model could only be fine-tuned with Nvidia RTX A6000 due to its large overhead of 1 billion parameters and also took the most amount of time to train.

3 Results and Discussion

3.1 Model Accuracy

Table 1: Accuracy metrics obtained from validation set inference on models fine-tuned with *Baseline* dataset for 25 epochs and *Prompt* dataset 2 epochs.

LLM	<i>Baseline</i> Fine-Tuned	<i>Prompt</i> Fine-Tuned
DistilBERT	88.41%	82.22%
SciBERT	90.88%	81.40%
T5	71.414%	88.13%
Llama	93.68%	73.52% ^a

^a Fine-tuned for 0.5 epochs instead of the full 2 epochs.

3.1.1 *Prompt* Fine-Tuned LLMs

Each of the LLMs were fine-tuned for 2 epochs with the exception of Llama where it was fine-tuned for only 0.5 epochs due to its lengthy training duration. Within the *Prompt* fine-tuned LLMs, the T5 model achieves the highest accuracy with DistilBERT and SciBERT achieving similar but lower accuracy results. Llama presents the lowest accuracy however this is with the caveat that it was fine-tuned for only half the dataset due to time constraints. With further training we would expect the achieved accuracy would be much higher, similar to that seen within the *Baseline* fine-tuned LLMs.

3.1.2 *Baseline* Fine-Tuned LLMs

Initially each of the LLM models were fine-tuned for 5 epochs on the *Baseline* dataset and further extended to 25 epochs with 5 epoch increments (Table 2) which resulted in all models apart from T5 showing significant improvement in evaluation accuracy. This was most prominently displayed in the Llama model where the extended training cycles drastically improved the model’s prediction accuracy, achieving an accuracy of 93.68%, the highest accuracy of all the trained models (Table 1). Llama’s higher accuracy is expected as its parameter size is over 9x greater (1 billion) to the BERT models which it is compared against (110 million) while taking also significantly more time to train as well. Notably, all models displayed plateauing or decreasing validation accuracy after 20 epochs indicating that further fine-tuning may not present additional benefit.

Table 2: Accuracy for models trained on *Baseline* dataset over a series of 25 epochs with 5 epoch increments.

LLM	5 Epochs	10 Epochs	15 Epochs	20 Epochs	25 Epochs
DistilBERT	84.22%	87.75%	87.75%	88.29%	88.41%
SciBERT	88.29%	88.93%	88.99%	91.32%	90.88%
T5	79.61%	71.45%	76.42%	77.92%	71.41%
Llama	89.18%	91.66%	92.94%	93.01%	93.68%

Of the four models trained with the *Baseline* dataset, the T5 model displayed the least

potential as its accuracy remained around 88% throughout all training epochs whereas all other models exhibited an improvement in evaluation accuracy. One reason for this could be attributed to the use of the T5-Small model which only consisted of 60 million parameters, the least of all compared models.²⁹ Its lightweight architecture and smaller dimensionality of 512 contribute to its lack of accuracy improvement after lengthening the number of training epochs.²⁹

Evaluating the performance of the *Prompt* dataset on LLMs fine tuned on the *Baseline* dataset, all exhibit poor performance. The initial expectation was that the large language models would be able to reason through input prompts and inherently map parameter values to those seen within the *Baseline* dataset. However with the high amount of defect misclassifications, the models seem to be highly dependent on the syntactical structure of process parameter inputs (Figure 5) of the *Baseline* dataset. Potentially adjusting the *Baseline* dataset to further include the names of each process parameter inside the input could help inform the model to the context of each value.

3.2 Principle Component Analysis

With the application of Principle Component Analysis (PCA) the model’s ability to distinguish between process parameters and their corresponding defects is more clearly defined. In PCA charts for LLM models fine-tuned with the *Baseline* datasets, a clear distinction can be defects for *Balling* and *Keyhole / Lack of Fusion*. Areas of *Keyhole* and *Lack of Fusion* share a greater amount of overlap and one explanation for this lies in the data augmentation procedure used to determine *Lack of Fusion* defects.

The PCA chart regarding the *Prompt* dataset (Figure 4) exhibits a different trend where all of the different defect regimes have high degrees of overlap on top of one another. This further supports the case that the LLMs fine-tuned on the *Baseline* dataset struggle to interpret the process parameters outlined in the *Prompt* dataset, most likely due to the fact that process parameters are not formatted in its expected syntax. As such, areas of *Keyhole*,

Lack of Fusion, *Balling*, and *None* have high degrees of overlap as the models fail to extract the significant features of each input.

4 Conclusion and Future Work

4.1 Conclusion

Analysis of fine-tuned LLM models show that the 1 billion parameter Llama 3 implementation achieves the highest accuracy of 93% on the *Baseline* dataset and T5 displays the highest comparable accuracy within the *Prompt* fine-tuned LLMs. It is worth noting that the Llama model presents a significantly longer training duration and parameter set than the other LLMs. With this it can be seen that larger parameter sets and lengthier training runs improve the evaluation accuracy of models fine tuned on the *Baseline* dataset. The findings here show that LLMs fine-tuned on a process parameter defect dataset are able to reason and predict potential defects existing in experimental and simulation data. The incorporation of natural language allows for a more accessible inputs enabling users to determine optimal build conditions with limited domain knowledge.

4.2 Future Work

Future work in this domain would focus upon obtaining a more diverse dataset with a wider range of materials, parameter sets, and additive processes. Longer fine-tuning of LLMs with the *Prompt* dataset could help expose the models to diverse input set of natural language and produce predictions with greater accuracy. In addition, parts of the existing models such as the tokenizer could be replaced with one better equipped in understanding numerical inputs.

4.3 Data Availability

The models and dataset are available within a HuggingFace collection at additivellm.ppak.net.

Acknowledgement

The author thanks Janghoon Ock for initial code reference and guidance on general aspects for training and performing inference on Large Language Models for domain specific tasks.

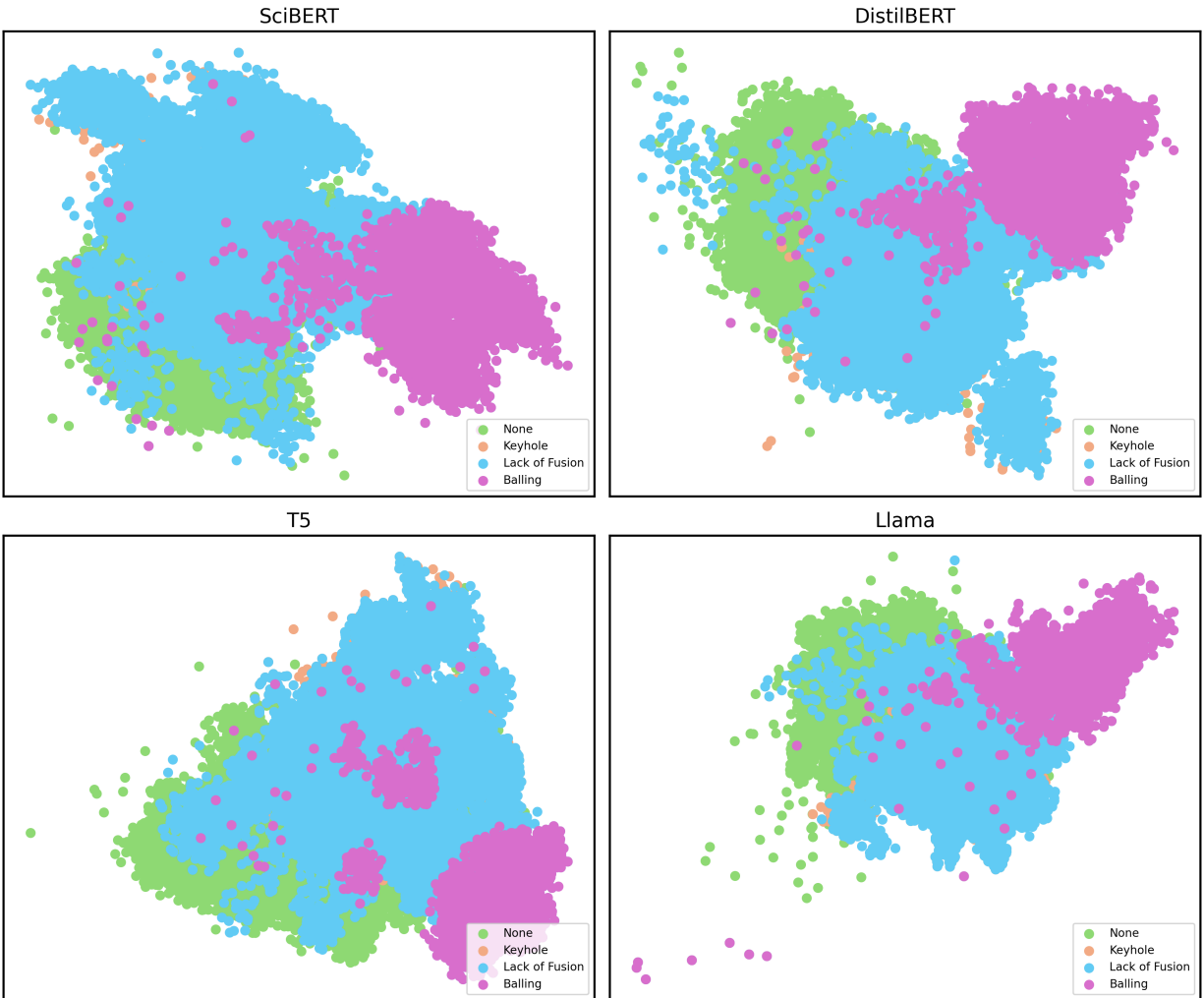


Figure 3: Principle Component Analysis (PCA) of LLMs fine-tuned (20 epochs) and evaluated with the *Baseline* dataset. For all models, the labels of *Keyhole* and *Lack of Fusion* share a high degree of overlap to the extent that *Lack of Fusion* covers much of the *Keyhole* labels.

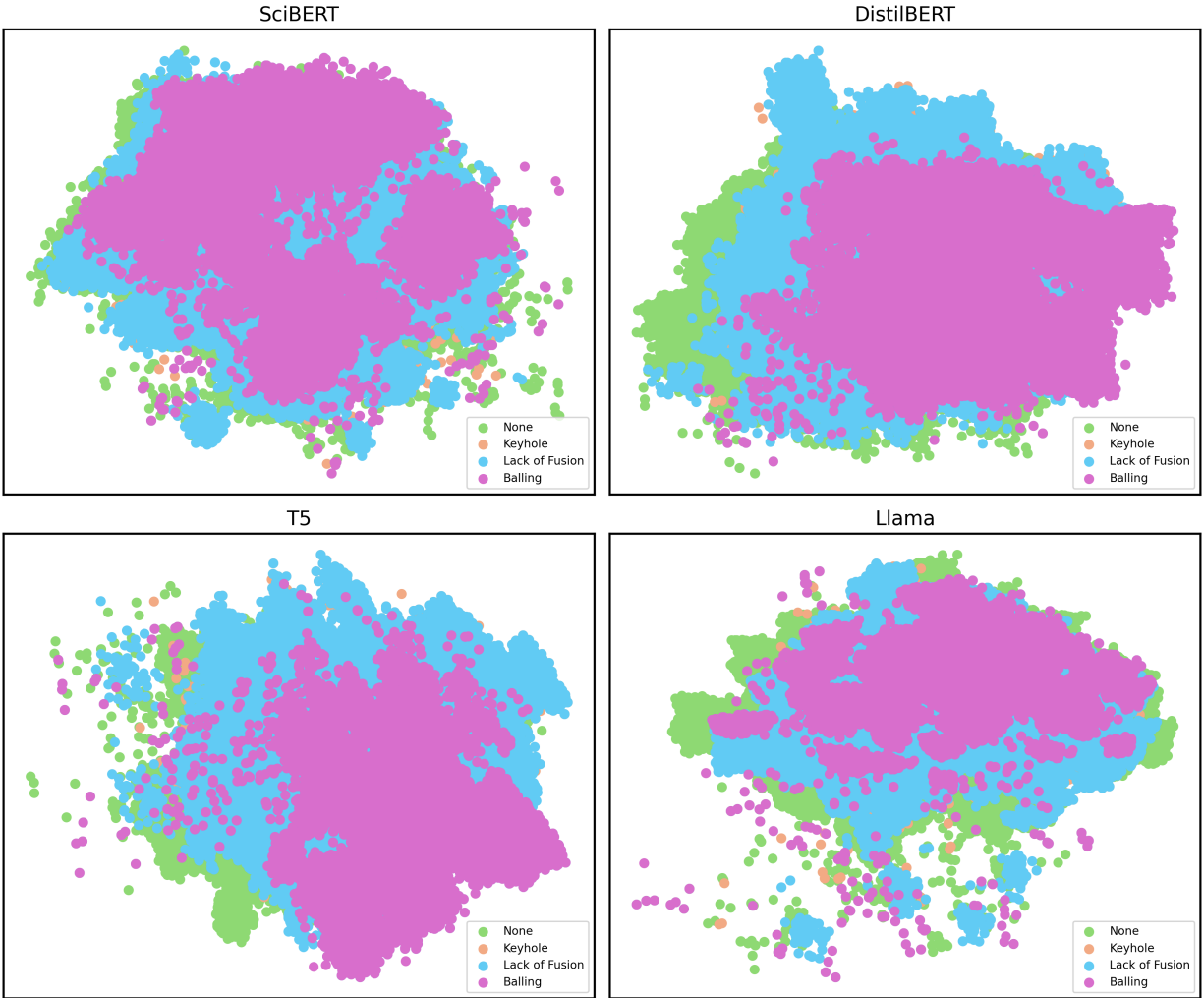


Figure 4: Principle Component analysis of LLM models fine-tuned on the *Baseline* dataset and inferred using the *Prompt* dataset show high degrees of over between all labels indicating the models struggle to extract relevant information when formatted in natural language.

Appendix A Dataset Templates

Baseline Template

```
<material>[SEP]<power>[SEP]<velocity>[SEP]<hatch_spacing>[SEP]<layer_height>[SEP]<beam_diameter>
```

Figure 5: The highlighted attributes are replaced with the appropriate values and corresponding units, unknown values are replaced with an empty string.

Prompt Template

```
Can you detail the potential imperfections that arise in <material> manufactured via L-PBF at <power>, utilizing a <beam_diameter> beam, traveling at <velocity>, with a hatch spacing of <hatch_spacing>, and a layer thickness of <layer_height>?
```

Figure 6: The text of each input label pair is formatted to a set of prompt templates, taking in consideration the multiple ways an input query can be structured.

References

- (1) Beuth, J.; Fox, J.; Gockel, J.; Montgomery, C.; Yang, R.; Qiao, H.; Soylemez, E.; Reeseewatt, P.; Anvari, A.; Narra, S.; Klingbeil, N. Process Mapping for Qualification Across Multiple Direct Metal Additive Manufacturing Processes. **2013**, Publisher: University of Texas at Austin.
- (2) Gordon, J. V.; Narra, S. P.; Cunningham, R. W.; Liu, H.; Chen, H.; Suter, R. M.; Beuth, J. L.; Rollett, A. D. Defect structure process maps for laser powder bed fusion additive manufacturing. *Additive Manufacturing* **2020**, *36*, 101552.
- (3) Ahmed, N.; Barsoum, I.; Haidemenopoulos, G.; Al-Rub, R. K. A. Process parameter selection and optimization of laser powder bed fusion for 316L stainless steel: A review. *Journal of Manufacturing Processes* **2022**, *75*, 415–434.
- (4) Roh, B.-M.; Kumara, S. R. T.; Witherell, P.; Simpson, T. W. Ontology-based Process Map for Metal Additive Manufacturing. *Journal of Materials Engineering and Performance* **2021**, *30*, 8784–8797.

- (5) Menon, N.; Mondal, S.; Basak, A. Multi-Fidelity Surrogate-Based Process Mapping with Uncertainty Quantification in Laser Directed Energy Deposition. *Materials* **2022**, *15*, 2902, Number: 8 Publisher: Multidisciplinary Digital Publishing Institute.
- (6) Huang, Y.; Fleming, T. G.; Clark, S. J.; Marussi, S.; Fezzaa, K.; Thiyagalingam, J.; Leung, C. L. A.; Lee, P. D. Keyhole fluctuation and pore formation mechanisms during laser powder bed fusion additive manufacturing. *Nature Communications* **2022**, *13*, 1170, Publisher: Nature Publishing Group.
- (7) Zhang, B.; Seede, R.; Xue, L.; Atli, K. C.; Zhang, C.; Whitt, A.; Karaman, I.; Arroyave, R.; Elwany, A. An efficient framework for printability assessment in Laser Powder Bed Fusion metal additive manufacturing. *Additive Manufacturing* **2021**, *46*, 102018.
- (8) Tang, M.; Pistorius, P. C.; Beuth, J. L. Prediction of lack-of-fusion porosity for powder bed fusion. *Additive Manufacturing* **2017**, *14*, 39–48.
- (9) Miner, J. P.; Ngo, A.; Gobert, C.; Reddy, T.; Lewandowski, J. J.; Rollett, A. D.; Beuth, J.; Narra, S. P. Impact of melt pool geometry variability on lack-of-fusion porosity and fatigue life in powder bed fusion-laser beam Ti–6Al–4V. *Additive Manufacturing* **2024**, *95*, 104506.
- (10) Gu, D.; Shen, Y. Balling phenomena during direct laser sintering of multi-component Cu-based metal powder. *Journal of Alloys and Compounds* **2007**, *432*, 163–166.
- (11) Touvron, H. et al. Llama 2: Open Foundation and Fine-Tuned Chat Models. 2023; <http://arxiv.org/abs/2307.09288>, arXiv:2307.09288.
- (12) Touvron, H.; Lavril, T.; Izacard, G.; Martinet, X.; Lachaux, M.-A.; Lacroix, T.; Rozière, B.; Goyal, N.; Hambro, E.; Azhar, F.; Rodriguez, A.; Joulin, A.; Grave, E.; Lample, G. LLaMA: Open and Efficient Foundation Language Models. 2023; <http://arxiv.org/abs/2302.13971>, arXiv:2302.13971.

- (13) Minaee, S.; Mikolov, T.; Nikzad, N.; Chenaghlu, M.; Socher, R.; Amatriain, X.; Gao, J. Large Language Models: A Survey. 2024; <http://arxiv.org/abs/2402.06196>, arXiv:2402.06196.
- (14) Devlin, J.; Chang, M.-W.; Lee, K.; Toutanova, K. BERT: Pre-training of Deep Bidirectional Transformers for Language Understanding. 2019; <http://arxiv.org/abs/1810.04805>, arXiv:1810.04805.
- (15) Brown, T. B. et al. Language Models are Few-Shot Learners. 2020; <http://arxiv.org/abs/2005.14165>, arXiv:2005.14165.
- (16) Liu, Y.; Ott, M.; Goyal, N.; Du, J.; Joshi, M.; Chen, D.; Levy, O.; Lewis, M.; Zettlemoyer, L.; Stoyanov, V. RoBERTa: A Robustly Optimized BERT Pretraining Approach. 2019; <http://arxiv.org/abs/1907.11692>, arXiv:1907.11692.
- (17) Jadhav, Y.; Pak, P.; Farimani, A. B. LLM-3D Print: Large Language Models To Monitor and Control 3D Printing. 2024; <http://arxiv.org/abs/2408.14307>, arXiv:2408.14307.
- (18) Ock, J.; Guntuboina, C.; Barati Farimani, A. Catalyst Energy Prediction with CatBERTa: Unveiling Feature Exploration Strategies through Large Language Models. *ACS Catalysis* **2023**, *13*, 16032–16044, Publisher: American Chemical Society.
- (19) Car, A.; Yarlagadda, S. S.; Bartsch, A.; George, A.; Farimani, A. B. PLATO: Planning with LLMs and Affordances for Tool Manipulation. 2024; <http://arxiv.org/abs/2409.11580>, arXiv:2409.11580.
- (20) Lorsung, C.; Farimani, A. B. Explain Like I’m Five: Using LLMs to Improve PDE Surrogate Models with Text. 2024; <http://arxiv.org/abs/2410.01137>, arXiv:2410.01137.

- (21) Shah, A.; Guntuboina, C.; Farimani, A. B. Peptide-GPT: Generative Design of Peptides using Generative Pre-trained Transformers and Bio-informatic Supervision. 2024; <http://arxiv.org/abs/2410.19222>, arXiv:2410.19222.
- (22) Farimani, A. B. Large Language Models Monitor and Control Additive Manufacturing. 2024.
- (23) Chandrasekhar, A.; Chan, J.; Ogoke, F.; Ajenifujah, O.; Farimani, A. B. AMGPT: a Large Language Model for Contextual Querying in Additive Manufacturing. 2024; <http://arxiv.org/abs/2406.00031>, arXiv:2406.00031.
- (24) Ock, J.; Badrinarayanan, S.; Magar, R.; Antony, A.; Barati Farimani, A. Multimodal language and graph learning of adsorption configuration in catalysis. *Nature Machine Intelligence* **2024**, 1–11, Publisher: Nature Publishing Group.
- (25) Balaji, S.; Magar, R.; Jadhav, Y.; Farimani, A. B. GPT-MolBERTa: GPT Molecular Features Language Model for molecular property prediction. 2023; <http://arxiv.org/abs/2310.03030>, arXiv:2310.03030 [physics].
- (26) Jadhav, Y.; Farimani, A. B. Large Language Model Agent as a Mechanical Designer. 2024; <http://arxiv.org/abs/2404.17525>, arXiv:2404.17525 [cs].
- (27) Ock, J.; Vinchurkar, T.; Jadhav, Y.; Farimani, A. B. Adsorb-Agent: Autonomous Identification of Stable Adsorption Configurations via Large Language Model Agent. 2024; <http://arxiv.org/abs/2410.16658>, arXiv:2410.16658 [cs].
- (28) Grattafiori, A. et al. The Llama 3 Herd of Models. 2024; <http://arxiv.org/abs/2407.21783>, arXiv:2407.21783 [cs].
- (29) Raffel, C.; Shazeer, N.; Roberts, A.; Lee, K.; Narang, S.; Matena, M.; Zhou, Y.; Li, W.; Liu, P. J. Exploring the Limits of Transfer Learning with a Unified Text-to-Text Transformer. 2023; <http://arxiv.org/abs/1910.10683>, arXiv:1910.10683 [cs].

- (30) Lan, Z.; Chen, M.; Goodman, S.; Gimpel, K.; Sharma, P.; Soricut, R. ALBERT: A Lite BERT for Self-supervised Learning of Language Representations. 2020; <http://arxiv.org/abs/1909.11942>, arXiv:1909.11942 [cs].
- (31) Sanh, V.; Debut, L.; Chaumond, J.; Wolf, T. DistilBERT, a distilled version of BERT: smaller, faster, cheaper and lighter. 2020; <http://arxiv.org/abs/1910.01108>, arXiv:1910.01108 [cs].
- (32) Radford, A.; Narasimhan, K.; Salimans, T.; Sutskever, I. Improving Language Understanding by Generative Pre-Training.
- (33) Beltagy, I.; Lo, K.; Cohan, A. SciBERT: A Pretrained Language Model for Scientific Text. 2019; <http://arxiv.org/abs/1903.10676>, arXiv:1903.10676 [cs].
- (34) meta-llama/Llama-3.2-1B · Hugging Face. 2024; <https://huggingface.co/meta-llama/Llama-3.2-1B>.
- (35) google-t5/t5-small · Hugging Face. 2024; <https://huggingface.co/google-t5/t5-small>.
- (36) Akbari, P.; Ogoke, F.; Kao, N.-Y.; Meidani, K.; Yeh, C.-Y.; Lee, W.; Barati Farihani, A. MeltpoolNet: Melt pool characteristic prediction in Metal Additive Manufacturing using machine learning. *Additive Manufacturing* **2022**, *55*, 102817.
- (37) FLOW-3D. <https://www.flow3d.com/>.
- (38) T5. https://huggingface.co/docs/transformers/v4.14.1/model_doc/t5.